

# Applications of the hollow-fibre infection model (HFIM) in viral infection studies

Japhette E. Kembou-Ringert <sup>1\*</sup>, John Readman<sup>1</sup>, Claire M. Smith<sup>1</sup>, Judith Breuer<sup>1</sup> and Joseph F. Standing <sup>1</sup>

<sup>1</sup>Department of Infection, Immunity & Inflammation, Great Ormond Street Institute of Child Health (ICH), University College London, 30 Guilford Street, London WC1N 1EH, UK

\*Corresponding author. E-mail: kjaphette@yahoo.fr

Conventional cell culture systems involve growing cells in stationary cultures in the presence of growth medium containing various types of supplements. At confluency, the cells are divided and further expanded in new culture dishes. This passage from confluent monolayer to sparse cultures does not reflect normal physiological conditions and represents quite a drastic physiological change that may affect the natural cell physiology. Hollow-fibre bioreactors were in part developed to overcome these limitations and since their inception, they have widely been used in production of monoclonal antibodies and recombinant proteins. These bioreactors are increasingly used to study antibacterial drug effects via simulation of *in vivo* pharmacokinetic profiles. The use of the hollow-fibre infection model (HFIM) in viral infection studies is less well developed and in this review we have analysed and summarized the current available literature on the use of these bioreactors, with an emphasis on viruses. Our work has demonstrated that this system can be applied for viral expansion, studies of drug resistance mechanisms, and studies of pharmacokinetic/pharmacodynamic (PK/PD) of antiviral compounds. These platforms could therefore have great applications in large-scale vaccine development, and in studies of mechanisms driving antiviral resistance, since the HFIM could recapitulate the same resistance mechanisms and mutations observed *in vivo* in clinic. Furthermore, some dosage and spacing regimens evaluated in the HFIM system, as allowing maximal viral suppression, are in line with clinical practice and highlight this ‘*in vivo*-like’ system as a powerful tool for experimental validation of *in vitro*-predicted antiviral activities.

## Introduction

Mammalian cell culture systems generally involve growing cells in stationary cultures in the presence of growth medium often supplemented with animal sera and other supplements. Once the cells have grown to confluency, they are expanded by several-fold subdivision and seeded into new culture dishes in the presence of new growth medium. By applying such conventional cell culture techniques, it has been possible to produce  $10^5$  to  $10^6$  cells/mL in growth medium. Common cell culture techniques are not often reflective of physiological cell growth conditions. Indeed, cell expansion by subdivision represents a sudden change in physiological conditions, where cells go from a confluent monolayer to sparse cell cultures. To address this limitation, Knazek *et al.*<sup>1</sup> developed the hollow-fibre bioreactor (HFB).

The HFB was originally a glass tube (in recent versions, the glass tube has been replaced by a polycarbonate shell) containing a bundle of selectively permeable hollow fibres attached to each end of the tube. The system has an inlet port and an outlet port that allows medium, from a central reservoir, to flow through the hollow fibres in a continuous loop. Typically, an

HFB (or cartridge) has two main compartments: an intracapillary space (ICS) within the hollow fibres, which brings in media and takes out waste, and an extracapillary space (ECS) surrounding the hollow fibres where the cells reside and grow (Figure 1). Cells are seeded into the bioreactor ECS through a sampling port located on the top of the bioreactor (see Figure 2 for an overview of the system). A detailed description of the system has been previously published by several authors.<sup>2–4</sup> Although the vast majority of HFB contain cellulosic fibres (for uniform cell expansion), HFBs can also contain polysulfone, polypropylene or polyethylene fibres.

The molecular weight cut-off (MWCO) of a cartridge module determines its retention abilities. The ‘useful retention’ (50% retention mark) is the size of protein that will be retained at  $\geq 90\%$  in the ECS. This retention also depends on the size, shape, post-translational modifications, and Stokes radius of the protein released into the ECS. For the 5 kDa MWCO fibres, the useful retention is  $\geq 20$  kDa and it is recommended for proteins in the range of 20 kDa up to about 140 kDa. For larger proteins, the 20 kDa MWCO fibre is recommended.<sup>5</sup>

This *in vitro* system offers a solution to culturing cells at high densities, from approximately  $2 \times 10^5$  to approximately

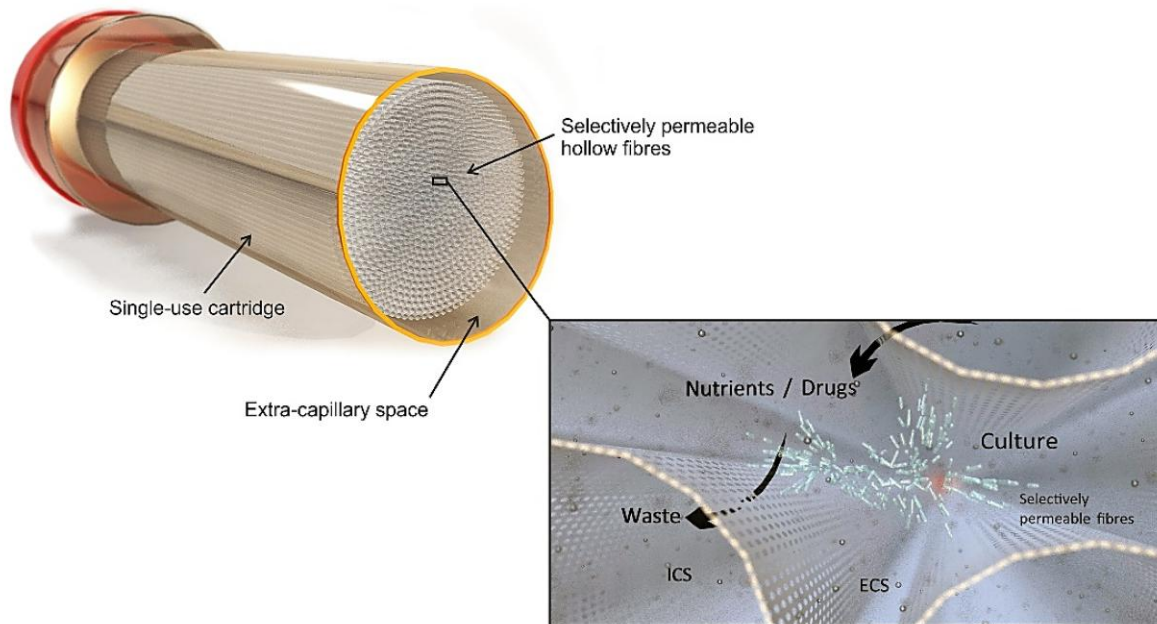


**Figure 1.** Cross-sectional image of a hollow-fibre cartridge, showing the two main compartments: the intracapillary space (ICS) within the hollow fibres, which brings in media (nutrients and antiviral drugs), and via which the waste is removed, and the extracapillary space (ECS), which is the space surrounding the fibres and where the cells are seeded for growth. This figure appears in colour in the online version of *JAC* and in black and white in the print version of *JAC*.

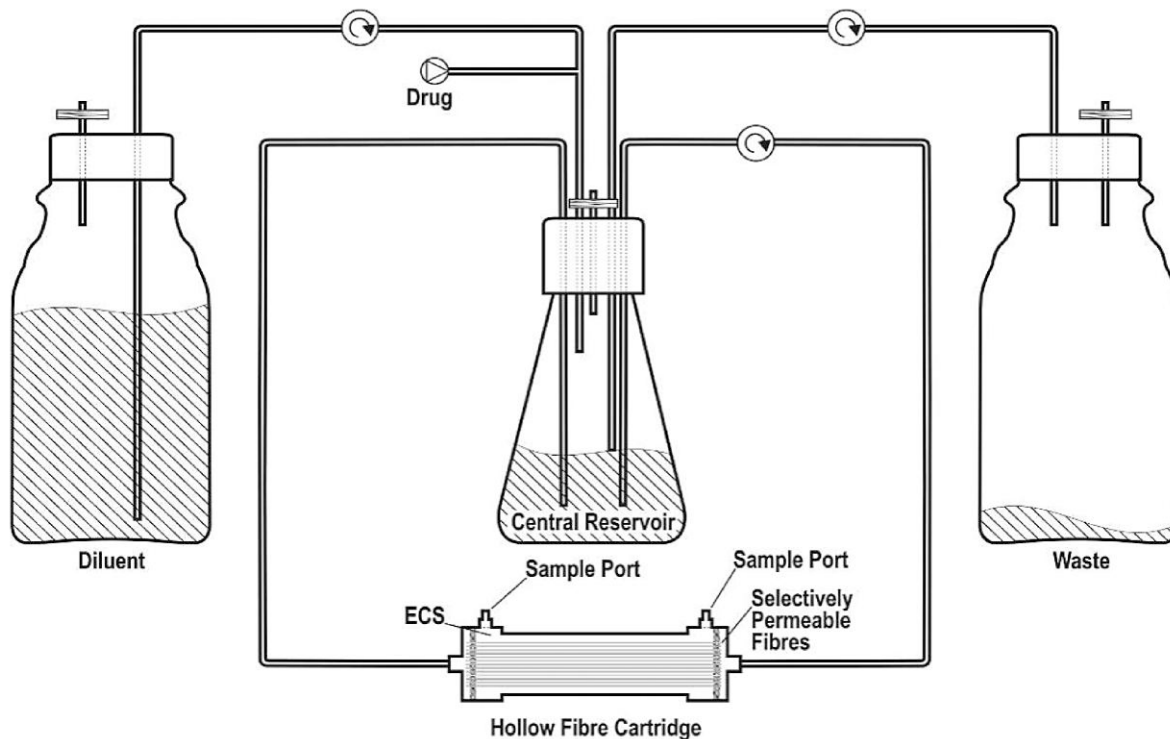


**Figure 2.** General overview of the HFIM system. The system is comprised of four main elements. The hollow fibre cartridge contains the selectively semi-permeable fibres on the outside of which (ECS) the cells are seeded for growth via the sampling ports. The fibres are terminally linked to a central reservoir, in which the media levels are kept constant by the action of a diluent reservoir (on the left) constantly topping up fresh media into the central reservoir and a waste removal tube taking out exhausted media to a waste reservoir (on the right). Antiviral drugs can be administered either to the diluent reservoir (continuous infusion) or to the central reservoir (IV bolus).

$1.7 \times 10^7$  over 28 days, as demonstrated for mouse L-929 fibroblast cells.<sup>1</sup> Since their inception, HFBs have widely been used in a different range of applications including cell propagation, production of monoclonal antibodies and production of recombinant proteins.<sup>6–9</sup>

In addition to supporting cell growth at physiological cell densities, this system offers several other advantages including growing cells for extended periods of time, and this is particularly important for pharmacodynamic (PD) and pharmacokinetic (PK) studies aiming at investigating cellular responses to drug exposure. Indeed, over recent years, the hollow-fibre infection model (HFIM) has been increasingly used to assess PK/PD indices of chemical compounds since the model allows drug profiling to be simulated.<sup>10–12</sup> The system is also relatively inexpensive compared with the cost inherent to clinical studies. Although *in vivo* animal models are well established and frequently used to test the effectiveness of antivirals, for ethical reasons they sometimes remain limited by the duration of the experiments to be carried out. Moreover, multiple animals need to be used in each arm for each timepoint, requiring ethically approved and well-established animal husbandry not often available in every research facility.

Most of the work done on the HFIM has focused on bacteria and antimicrobial testing.<sup>11,13–15</sup> Although comprehensive literature on the use of the HFIM for performance evaluation of antimicrobial compounds exist,<sup>16–20</sup> the current literature about

the applications of the HFIM to study viral infections is still lacking. This review therefore focuses on the applications of the HFIM in viral infection studies. By summarizing the different infection approaches and readouts described in the available literature when using this system, our work aims at providing researchers in this field with some of the necessary technical knowledge surrounding the use of this system when applied to viral infections.

## Viral expansion studies

As previously mentioned, one of the key benefits of HFBs is the ability to grow cells at high densities. The system can sustain the growth of up to  $10^9$  cells.<sup>21,22</sup> The continuous medium that perfuses through the HFB both feeds the cells and removes toxic waste, which in turn promotes continuous cell growth. This advantage of sustaining high cell densities therefore allows for the system to be used for optimal virus production.

Most viral expansion studies performed in the HFIM system appear to require a high inoculum multiplicity of infection or MOI (between 5 and 10) to initiate the infection. In addition, viral yields can be assessed using various virology methods such as plaque assay, TCID<sub>50</sub>, fluorescent focus assay, ELISA (to quantify a specific viral antigen), quantitative RT-PCR (qRT-PCR) (for total viral RNA) or flow cytometry of virus-infected cells, to determine

**Table 1.** Practical aspects of the HFIM system for eukaryotic virus infections

Aspects	Specifications
Types of study	Viral expansion, drug resistance, PK/PD (dose-range, dose-fractionation) studies
Duration of the study	Cells can be maintained for up to 69 days (more than 2 months) in the HFIM system <sup>23</sup>
Choice of the cartridge	Types of fibre MWCO
Characteristics of the cell line	Most studies have reported using polysulfone cartridges, but cellulose cartridges have also been successfully used for PK/PD studies <sup>24–26</sup> 5 kDa MWCO for smaller size selection, 20 kDa MWCO for larger size selection
moi	Both adherent cells and cells grown in suspension have been reported and successfully used Differs according to the type of studies: high moi (5–10) has mostly been reported for viral expansion studies, while low moi (mostly 0.001) has been reported for both drug resistance and PK/PD studies
Read-out for viral burden	Plaque assay and TCID <sub>50</sub> (for infectious virus), fluorescent focus assay, ELISA (for specific viral antigen, e.g. HIV P24), qRT-PCR (for total viral RNA), flow cytometry (of virus infected cells, to determine the % of viral antigen-positive cells—more practical for cells grown in suspension)
Monitoring cell growth in the bioreactor ECS	Glucose consumption, lactate production
Monitoring antiviral drug concentration within the system (for PK/PD and drug resistance studies)	LC-MS/MS
Route of drug administration	To the diluent reservoir (to simulate continuous infusion) or the central reservoir (to simulate IV bolus).
Choice of culture media	Serum-free media (mostly reported for viral expansion studies), Virus growth media (VGM—the composition varies according to growth requirements of the cells and the infectivity conditions of the virus under study) Drug-containing VGM (for drug resistance and PK/PD studies).

the percentage of viral antigen-positive cells (as summarized in Table 1).

Plaque assay and TCID<sub>50</sub> (or endpoint dilution) are both viral quantification methods used to determine the number of infectious viral particles in a given preparation (viral titre). Although both methods assess the number of infectious viral particles in a given preparation, TCID<sub>50</sub> is more commonly used when the infection results in the destruction of the cell monolayer without plaque formation. Fluorescent focus assay is another alternative to plaque assay, used to determine the titre of viruses that do not form plaques. This method relies on the immunostaining detection of fluorescent virus-infected foci (similar to plaques) using antibodies raised against a specific viral protein. When the gene encoding a fluorescent protein is incorporated into the viral genome, foci can be detected without the use of antiviral antibodies. While qRT-PCR is used to quantify the total amount of virus (both infectious and non-infectious) resulting from an infection using total viral RNA as the starting material, flow cytometry, on the other hand, is used to determine the percentage of viral antigen-positive cells within an infected cell population.

The choice of the readout for viral burden will therefore depend on the characteristics of the virus used (cytopathic virus forming plaques versus non-cytopathic virus), the availability of antibodies specific to the virus (to allow its immunodetection), or the level of precision when reporting the amount of virus quantified (total virus versus number of infectious virus versus percentage of viral antigen-expressing cells).

Using 293 cells adapted to grow in suspension, Gardner *et al.*<sup>27</sup> used the HFIM to produce high titres of recombinant adenovirus in serum-free medium. In this study, the authors used three different approaches to infect the cells in the HFB (30 kDa MWCO cellulosic fibre module). In a first approach, the cells were inoculated into the ECS of the bioreactor and allowed to grow for 5 days before the infection was carried out by injecting the virus into the ECS through the sampling ports. The second approach consisted of allowing the cells to equilibrate in the ECS for 24 h, to then be similarly infected through the sampling ports. The third approach consisted of co-inoculating the cells with the virus to allow the infection to then proceed. In these three cases, the cells and virus were harvested 3 days post infection for virus purification and quantification using the methods described by Graham and Prevec.<sup>28</sup> Given the fact that the HFB is a closed system, meaning that most cellular processes cannot be visualized, Gardner *et al.*<sup>27</sup> used lactate production to monitor cell growth within the bioreactor. Although it is unclear if lactate production was quantified in the ECS or in the central reservoir, cells and virus were harvested when lactate production showed a sharp fall-off. All three infection approaches generated similar virus yields of approximately  $2.4 \times 10^{13}$  infectious viral particles (total virus quantified from four cartridges) with about  $5 \times 10^8$ – $10 \times 10^8$  cells infected at an MOI between 5 and 10.

Leong *et al.*<sup>21</sup> used a slightly different approach to expand HIV-1 in co-cultures of primary human PBMCs. For infections in the HFB,  $7 \times 10^8$  phytohaemagglutinin (PHA)-stimulated PBMCs were mixed with HIV-1, incubated for 2 h to allow viral adsorption, resuspended in culture medium, and inoculated into the ECS of a 20 kDa MWCO HFB. The cultures were then incubated at 37°C for 7–10 days before culture supernatants were harvested. HIV yields were measured in terms of the amount of

p24 antigen detected by enzyme immunoassay (EIA) on cell-free culture supernatants.

Similarly to Gardner *et al.*,<sup>27</sup> Leong *et al.*<sup>21</sup> used lactate production, sampled daily from the reservoir, to monitor cell growth within the HFB (although it is also not clear in this case if lactate production was quantified in the ECS or in the central reservoir). By comparing varying concentrations of IL-2, FBS and glucose content in the medium, the authors were able to establish that PBMC cultures in 20 kDa MWCO cartridges with 15% FBS, 80 IU/mL IL-2 and 2.0 g/L glucose generated the highest p24 yield of about 34.29 µg. Although the authors successfully established that the HFIM can support substantial HIV-1 growth in human primary PBMCs under optimal conditions, it would have been interesting to know how p24 viral yields translated to actual number of infectious viral particles, which is one drawback in this study. Interestingly, the authors found that 5 kDa MWCO bioreactor cartridges generated lower p24 yields than 20 kDa MWCO cartridges, suggesting that the choice of the MWCO of the cartridge might have an impact on the viral yield. Some preliminary experimental work to test the suitability of cartridges of different MWCOs are therefore encouraged.

Viral expansion in HFBs has also been performed by Hirschel *et al.*<sup>22</sup> for influenza A virus (IAV). The authors have shown that by infecting adherent MDCK cells with IAV (strain A/Mexico/4108/2009 H1N1), it was possible to obtain infectious virus concentrations of up to  $3 \times 10^9$  virions/mL (with total virus concentrations ranging from  $1 \times 10^{10}$  to  $1 \times 10^{11}$  virions/mL). In this study,  $1 \times 10^8$  cells were inoculated into the ECS of an HFB and allowed to attach to the hollow-fibre membranes for 14 days until the total number of cells reached approximately  $1 \times 10^9$ . Subsequently, 100 virus-infected MDCK cells, in a 5 mL volume of medium, were introduced into the ECS of the bioreactor. Following viral infection, 0.5 mL of the ECS was sampled daily and assayed for infectious virus by plaque assay.

To follow up with the work of Hirschel *et al.*,<sup>22</sup> Tapia *et al.*<sup>29</sup> compared the production of IAV in both adherent and suspension MDCK cells cultured in HFBs. The authors used a similar approach to the one described by Gardner *et al.*<sup>27</sup> Briefly, MDCK and MDCK SUS2 cells were seeded into the ECS of HBRs. Cells were allowed to grow for approximately 5 days. When maximum glucose uptake was observed, the cells were infected with either A/Puerto Rico/8/34 (H1N1) or A/Mexico/4108/2009 (H1N1) at an MOI of 0.001. Viral production was monitored daily by TCID<sub>50</sub> and haemagglutinin titres. By applying these procedures, Tapia *et al.*<sup>29</sup> reported viral titres of up to  $8.11 \times 10^{12}$  (total virions) and  $2.10 \times 10^{13}$  (total virions) for both MDCK adherent and MDCK SUS2 cells, respectively. Interestingly, cells could be cultured in the ECS of HFBs for up to 27 days (this included cell growth and infection time). For some of the experiments, the authors even describe a multiple harvest strategy during which the supernatant of the ECS could be harvested up to 14 times, therefore confirming the suitability of HFBs for long-term viral studies.

High-yield production of HCV was also achieved in a study conducted by Pihl *et al.*,<sup>30</sup> in which the authors were able to grow Huh 7.5 cells in the HFBs for up to 69 days. By employing a multiple harvest strategy, Pihl *et al.*<sup>30</sup> could recover a total harvest of up to  $2.7 \times 10^9$  focal-forming units (ffu)/mL at the end of the study, with peak HCV infectivity titres of up to  $7.6 \log_{10}$  ffu/mL (on Day 26 post seeding) using HFB cartridges of MWCO 20 kDa.

Although the authors remained consistent in the number of FFU used for infections in the HFBs ( $1.25 \times 10^6$  ffu), it was not clear throughout the study as to why there was a variation in the number of cells seeded in the cartridges for each hollow-fibre infection experiment. Nevertheless, this study revealed interesting findings related to the biological characteristics of HCV virions recovered from the HFBs (discussed in further detail below), which have not been addressed by other studies so far.

Overall, HFBs appear to be ideal platforms for high-yield production of viruses in both adherent and non-adherent cells. These platforms can therefore have great application potential in vaccine development, large-scale amplification and production of vaccines, especially inactivated vaccines, live attenuated vaccines, protein subunit vaccines, virus-like particle vaccines and replicating viral vector vaccines.

## Drug resistance studies

As previously mentioned, HFBs can sustain the growth of cells at high densities for weeks and even months.<sup>23,29,30</sup> This feature makes these cell culture platforms very useful models for the study of viral infections focusing on drug resistance generation and monitoring. In fact, the HFIM system can be used to identify both early and late mutations arising from drug exposure to specific antivirals. Selection of drug-resistant viruses under antiviral drug pressure is gaining ground and has been reported for many viruses.<sup>31</sup> Given the limitations of animal models for long-term studies, developing experimental systems that can model the selection of resistant virus species under drug pressure, as often observed in humans, is of paramount importance, as this could allow researchers to explore the spacing of doses as well as the administration schedule of antiviral drugs to determine if the emergence of resistance can be suppressed.

Brown *et al.*<sup>32</sup> used the HFIM system to model IAV resistance under drug pressure. To examine the effect of amantadine on the replication of IAV A/Albany/1/98 (H3N2),  $10^2$  IAV virus-infected MDCK cells were mixed with  $10^8$  uninfected cells and seeded in the ECS of HFBs. Each unit was then continuously infused with different concentrations of amantadine for 6 to 7 days. The ECS of the HFBs was sampled daily and assayed for infectious virus by plaque assay and for genomic viral RNA by real-time qRT-PCR. The authors also used HPLC tandem MS (LC/MS/MS) to determine, monitor and confirm the concentrations of amantadine present in both the ECS and the ICS of each HFB at different timepoints throughout the experiments. To identify mutations related to selective pressure due to the use of amantadine, the M2 gene of the progeny virus, sampled from the ECS of the HBRs, was sequenced.

Since continuous infusions of drug concentrations, representing AUC<sub>0-24</sub> of 7.2, 19.2, 48 and 144 mg·h/L daily doses, failed to suppress virus replication, Brown *et al.*<sup>32</sup> exposed MDCK cells, in the HFBs, to simulated concentrations equivalent to oral clinical doses of 66, 200 and 660 mg of amantadine once a day. The drug was initially given as an infusion over 1 h, which was then followed by a no-drug washout period resulting in a peak/trough concentration profile mimicking oral clinical exposure. The effect of these drug concentrations on virus replication was then determined by plaque assay (for infectious virus) and qRT-PCR. In this study, the authors were able to identify mutations in the M2 gene

that were identical to those reported in clinical isolates. One major (and of interest) conclusion from these experiments is that the HFIM system is indeed a suitable model to capture and study the emergence of resistant mutant virus (as occurring in the host, under drug selection). Although the simulated drug regimens used in this study failed to prevent the emergence of IAV resistance to amantadine, even at higher drug concentrations, these data by Brown *et al.*<sup>32</sup> highlight the HFIM system as a relevant system that can allow the modelling and study of mechanisms driving clinically observed antiviral resistance.

A drug resistance study was also conducted by Pihl *et al.*<sup>30</sup> to assess HCV escape from the direct-acting antiviral (DAA) daclatasvir (a drug targeting HCV NS5A). In this work, the Huh 7.5 cells were infected with HCV 5 days post seeding in the HFB. On Day 9 post seeding, serum-containing medium was exchanged for serum-free medium, and the virus was harvested every 2 days. Daclatasvir was then added to the medium on Day 27 at a concentration of  $64 \times EC_{50}$  and maintained in the medium at that concentration for over 18 days. Drug concentration was then increased to  $1024 \times EC_{50}$  and maintained in the medium for an additional 14 days, after which the treatment was terminated at Day 59 post seeding. Determination of HCV infectivity titres by fluorescent focus assay revealed that daclatasvir treatment did inhibit HCV infectivity (as demonstrated by the strong decrease in the amount of infectious HCV particles detected) following treatment initiation. Intriguingly, HCV viral RNA levels (measured by qRT-PCR on RNA extracted from the harvested supernatants) remained constant throughout the treatment, which suggests that the treatment did not prevent virus production but caused most virions produced to become non-infectious. Following the increase of the treatment concentration from  $64 \times EC_{50}$  to  $1024 \times EC_{50}$ , the authors interestingly observed the emergence of an NS5A-Y93H substitution (assessed by direct sequence analysis), which conferred HCV escape variants a 2645-fold resistance to daclatasvir, suggesting that lower doses may avoid the emergence of resistance.

Although the exact mechanisms by which this resistance occurred remains unclear, one possible explanation could be the fact that the increasing dose of drug exerts a selective pressure on viruses, which in turn develop mutations including those which confer them resistance to the antiviral drug. The viruses harbouring these mutations allowing them to escape drug pressure are then eventually selected for and begin to accumulate. This has been documented with oseltamivir for influenza viruses, with protease inhibitors such as amprenavir and saquinavir used for HIV treatment, and with cidofovir used for the treatment of vaccinia virus.<sup>33</sup> Optimization of drug combinations is thus a clinically promising approach to address such drug resistance when multiple drug classes exist against a specific virus.

Few other studies that have assessed antiviral pharmacokinetics and pharmacodynamics (discussed in the PK/PD section) have also simultaneously assessed viral drug resistance in the HFIM system. As discussed in a later section of this review, Pires de Mello *et al.*<sup>34</sup> for instance, have used the HFIM to demonstrate that the oseltamivir/zanamivir combination can effectively suppress drug-resistant H1N1 IAV, whereas in a similar study carried out by Brown *et al.*,<sup>35</sup> it was found that a 600 mg twice-daily regimen of zanamivir could inhibit oseltamivir-resistant 2009

pandemic H1N1 influenza virus in the HFIM system. These studies are further discussed in the PK/PD section.

In the light of the above studies, it clearly appears that the HFIM can allow the emergence of drug-resistant mutant virus, harbouring mutations similar to those reported in clinics, to be captured as well as drug resistance under drug pressure to be studied. This system can equally allow the screening of antiviral doses favouring the emergence of such drug-resistant mutations. All of this could have a significant clinical impact on prescribed drug regimens for major viruses of human importance.

### Antiviral PK/PD (dose-range and dose-fractionation) studies

According to Mehrotra *et al.*,<sup>36</sup> pharmacokinetics (PK—‘what the body does to the drug’) describes the time course of the concentration of a drug in a body fluid (plasma or blood) that results from the administration of a certain dosage regimen. Pharmacodynamics (PD—‘what the drug does to the body’), on the other hand, describes the intensity of a drug effect in relation to its concentration in a body fluid, usually at the site of drug action.<sup>36</sup>

The HFIM system has the advantage that it is a highly controlled system. Multiple variables such as dosing and drug administration time can be accurately adjusted. This makes it possible to precisely simulate a specific dosage regimen, allowing pharmacodynamics to be studied under *in vivo* equivalent pharmacokinetic conditions.

PK/PD studies using the HFIM system have been performed for viruses such as IAV, HIV and Zika virus and for most of these studies, the pharmacodynamically linked index of the compound being evaluated was determined by first determining the EC<sub>50</sub> value of this compound *in vitro* in flasks. A dose-range study was then performed in the HFIM system to identify the daily exposure (or exposure target) that will have a known antiviral effect in the HFIM system. Alternatively, the exposure target, either C<sub>max</sub> (the maximum concentration), AUC<sub>0–24</sub> (area under the concentration–time curve from 0 to 24 h), or C<sub>min</sub> (minimum concentration), is determined in a dose-fractionation study where, for example, one hollow-fibre unit receives the drug at the desired concentration in a continuous infusion manner, whereas other hollow-fibre units receive the drug as boluses (either single or broken up into several equal parts) followed by a no-drug washout. This results in a range of C<sub>max</sub>, AUC and C<sub>min</sub> values with drug concentrations usually set to mimic the half-life of the compound *in vivo*.<sup>37</sup> Time above a threshold such as EC<sub>50</sub> or EC<sub>90</sub> can also be calculated in washout experiments using pump settings and/or measured pharmacokinetics to predict the concentration–time course. Results from dose-fractionation experiments often determine the pharmacodynamically linked index of the antiviral compound for the virus under study.

The effect of the drug on the yield of cell-free virus (or virus replication) can then be determined by sampling the ECS of the bioreactor daily, measuring the amount of released virus by plaque assay or by ELISA (to determine the amount of viral antigen produced in the bioreactor over time). In addition, drug effect on virus replication can also be determined by sampling the ECS content and by counting the number of virus-infected cells by fluorescence-activated cell sorting (FACS) analysis of cells treated

with fluorochrome-labelled monoclonal antibody to a specific viral antigen of the virus under study.<sup>37</sup> Liquid chromatography with tandem MS (LC/MS/MS) can be used to determine and monitor the actual concentration of antiviral drug in both the central reservoir and the ECS.

### Influenza A virus (IAV)

Since the current clinically recommended dose and schedule of oseltamivir for the treatment of influenza in adults are 75 mg given twice a day, McSharry *et al.*<sup>38</sup> set out to examine whether there was a change in drug effect if the total dose (150 mg) was administered once a day. The authors used the HFIM system to determine the drug susceptibility and the pharmacodynamically linked variable of oseltamivir for influenza virus A/Sydney/5/97 (H3N2). Once the authors had determined the EC<sub>50</sub> value of oseltamivir (in flasks) to be 10.23 ± 8.66 ng/mL, they performed a dose-ranging study in the HFIM system. For this, 10<sup>2</sup> infected AX-4 cells (a derivative of MDCK cells transfected with the human β-galactoside α-2,6-sialyltransferase 1 gene) were mixed with 10<sup>8</sup> uninfected AX-4 cells and loaded in the ECS of six hollow-fibre units. The units were infused with various concentrations of the drug (0.1, 1, 10, 100 and 1000 ng/mL) in virus growth medium for 6 days. The effect of the drug on virus replication was determined daily by both plaque assay and haemagglutination assay, performed on supernatants collected from the ECS. To then determine the PK/PD index of oseltamivir, the authors performed a dose-fractionation study, during which one hollow-fibre unit received an exposure equivalent to 1 ng/mL (corresponding to an AUC<sub>0–24</sub> of 24 ng·h/mL) delivered by continuous infusion. A second hollow-fibre unit received the same exposure once a day (1 h infusion every 24 h). The third unit received the same exposure twice a day (two equal fractions every 12 h) whereas a fourth unit received the same exposure three times a day (three equal fractions every 8 h). Each infusion dose was followed by a no-drug washout to produce the appropriate half-life for this drug. The effect of the drug on virus replication was determined by sampling the units daily to measure the amount of released virus by both plaque assay and haemagglutination assay. Drug concentrations in each HFIM system were monitored at various times by LC/MS/MS. Results from the dose-fractionation study revealed that all treatment arms effectively suppressed virus replication to the same extent, indicating that the PK/PD index for oseltamivir for the IAV R292 strain is the AUC<sub>0–24</sub>/EC<sub>50</sub> ratio; although this finding remains to be clinically verified, it also suggests that it could be possible to treat influenza virus infection once daily with a dose of 150 mg/day.

A similar pharmacodynamics study was performed by Brown *et al.*<sup>35</sup> to predict optimal dosing regimens for zanamivir against an oseltamivir-resistant [HK/09-H275Y] 2009 pandemic H1N1 (pH1N1) influenza virus strain. The authors determined the EC<sub>50</sub> of zanamivir for this IAV strain to be 0.05 ng/mL. To determine if a once-a-day administration and/or lower doses of zanamivir could effectively suppress oseltamivir-resistant pH1N1 HK/09-H275Y viral replication to similar levels as the clinically recommended dosing regimen, Brown *et al.*<sup>35</sup> performed a dose-range and fractionation study in which average exposures to zanamivir at 1200, 600 or 300 mg administered once a day (q24h) or average exposures at 600, 300 or 150 mg administered twice daily

(q12h) were simulated over a 5 day period in hollow-fibre units containing  $10^2$  A/Hong Kong MDCK-infected cells mixed with  $10^8$  uninfected cells. All dose regimens were followed by a no-drug washout to simulate the human half-life of 2.5 h and LC/MS/MS was used to monitor zanamivir concentrations in the central reservoir throughout the infections. All q12h regimens suppressed viral replication better than q24h regimens. Moreover, q12h dosage regimens resulted in sustained dose response throughout the course of infection, with the 600 mg q12h dose regimen yielding maximal suppression of virus replication, therefore demonstrating that zanamivir can indeed inhibit the replication of oseltamivir-resistant pH1N1 HK/09-H275Y virus in MDCK cells. The fact that q12h regimens inhibited viral replication to a greater extent than q24h regimens suggests that the pharmacodynamically linked index of zanamivir for the HK/09-H275Y IAV is the time for which the level of the drug is above the  $EC_{50}$  ( $T_{>EC_{50}}$ ). This study is therefore in line with clinical practice and highlights the fact that clinical administration of IV zanamivir at a 600 mg q12h dosage is indeed sufficient to treat patients infected with oseltamivir-resistant influenza viruses.

The efficacy of combination therapy at suppressing IAV infections in the HFIM system was also demonstrated by Pires de Mello *et al.*<sup>34</sup> In this study, the authors evaluated the efficacy of oseltamivir/zanamivir combination therapy at suppressing drug-resistant HK/09-H275Y H1N1 IAV in the HFIM system. Oseltamivir and zanamivir are neuraminidase inhibitors both targeting the same viral protein (the neuraminidase of influenza viruses) although via different binding mechanisms. The evaluation of such a combination therapeutic approach could be clinically beneficial, especially when considering the growing emergence of antiviral drug resistance and the absence of novel antiviral compounds targeting resistant influenza viruses. In this study,  $10^2$  plaque forming units (pfu) of virus were mixed with  $10^8$  uninfected MDCK cells and resuspended in 25 mL of viral growth medium. The virus-containing cell suspension was inoculated into the ECS of hollow-fibre cartridges. Oseltamivir q12h (75 mg twice a day) and zanamivir q12h (600 mg twice a day) were delivered into the hollow fibres as a 1 h infusion monotherapy or in combination, and daily viral burden was assessed by plaque assay on MDCK cells. To ensure the correct concentrations of oseltamivir and zanamivir were delivered to the hollow-fibre cartridges, drug concentrations in the central reservoir were quantified by HPLC/MS/MS. Zanamivir alone (regardless of exposure) effectively suppressed HK/09-H275Y and provided sustained viral suppression by reducing peak viral titres by approximately  $4 \log_{10}$  pfu/mL. Combination therapy, on the other hand, also displayed substantial antiviral activity against HK/09-H275Y and was as effective as zanamivir alone. In fact, all zanamivir-containing regimens (the clinical monotherapy exposure of 600 mg twice daily, high monotherapy exposure and oseltamivir/zanamivir combination regimen), prevented the replication of drug-resistant HK/09-H275Y throughout the entire study (5 days). The effectiveness of this combination regimen against oseltamivir-resistant viruses makes this drug combination approach a rather beneficial treatment strategy over standard monotherapy regimens, since the current clinical regimen of oseltamivir (75 mg twice a day) appears to rapidly select for oseltamivir-resistant virus subpopulations in a mixed viral infection. Since oseltamivir/zanamivir combination was able to

suppress the selection of oseltamivir-resistant viruses and prevent their replication in a mixed infection model, this approach could clinically translate into using fewer doses of both drugs, while achieving the maximal viral suppression that will prevent the spread of drug-resistant strains.

### **Human immunodeficiency virus (HIV)**

Over the past years, several PK/PD HFIM system studies have been performed to test the efficacy of a wide range of antivirals acting against HIV.

One of these studies involved HIV-1 and the integrase inhibitor raltegravir. Raltegravir is clinically administered as a 400 mg twice-daily dose. Once bound, the drug remains in the active site of HIV-1 integrase protein for a long time, suggesting that once-a-day dosing of 800 mg may be as efficacious as the recommended regimen of 400 mg twice a day. Brown *et al.*<sup>39</sup> therefore set out to identify the PK/PD determinants for raltegravir that allow for a once-a-day regimen. For dose-ranging studies,  $10^9$  H9 cells infected with HIV IIIB were mixed with  $10^8$  uninfected CEM-SS cells and inoculated into the ECS of six polysulfone hollow-fibre cartridges. Raltegravir was then administered as a continuous infusion into five hollow-fibre cartridges, with one cartridge serving as the no-treatment control. The ECS of each cartridge was sampled daily for 6 days and the percentage of HIV antigen-positive cells was determined by flow cytometry analysis. In these dose-ranging studies, raltegravir inhibited cell-to-cell viral spread in a dose-dependent manner without completely suppressing viral spreading. The  $EC_{50}$  was determined to be 7.43 ng/mL. For dose-fractionation studies,  $10^6$  H9 cells infected with HIV IIIB were mixed with  $10^8$  uninfected CEM-SS cells and inoculated into the ECS of nine hollow-fibre cartridges. Raltegravir was then administered as a 1 h infusion. Four cartridges received the total exposure once daily (q24h) and four cartridges received half the daily exposure twice daily (q12h). One cartridge did not receive drug and served as the no-treatment control. Half-lives of 8, 4, 3 and 2 h were simulated and the percentage of p24 antigen-positive cells was determined by flow cytometry. According to the results from dose-fractionation studies, the antiviral activity of raltegravir was similar between q24h and q12h dosing regimens when pharmacokinetic profiles with longer half-lives of 8 versus 4 h (thus smaller clearance values) were simulated. Moreover, more frequent dosing (shorter dosing intervals) appeared to be required to provide maximal viral suppression for pharmacokinetic profiles with shorter half-lives (larger clearance), meaning that for maximal viral suppression with shorter half-lives, raltegravir concentrations must remain above the  $EC_{90}$  value for at least 57% of the time for a 24 h period or free-drug trough concentrations must be  $>3$  ng/mL. Although viral inhibition was similar between q24h and q12h dosage regimens at 8 and 4 h half-lives, the q24h regimen was found to be not as efficacious as the q12h regimen when shorter half-lives were simulated. Hence the clinical dose frequency of q12h is recommended to account for interindividual variability in raltegravir pharmacokinetics.

Another antiviral tested against HIV was the protease inhibitor A-77003. In this study by Bilello *et al.*,<sup>40</sup> four HFBs were loaded with a mixture of  $3.5 \times 10^5$  CEM-H9<sub>IIIB</sub>-infected cells and  $3.5 \times 10^7$  uninfected CEM cells. One hollow-fibre unit served as the no-

drug control while the others received continuous infusion of 0.063, 0.125 and 0.25  $\mu\text{M}$  A-77003 (representing 0.5-, 1- and 2-fold of the  $\text{EC}_{50}$  of 0.124  $\mu\text{M}$  previously estimated in flasks respectively) for 11 days. The continuous infusion regimens were simulated by adding A-77003 at the indicated concentrations directly to the medium circulating in the central reservoir. Hollow-fibre units were sampled daily and the A-77003 effect on viral replication was assessed by p24 ELISA. Although A-77003 showed a dose-response over time, the compound failed to completely inhibit virus replication, even at higher concentration of 0.25  $\mu\text{M}$ . To determine a drug concentration that can effectively inhibit HIV infection and virus spreading, Bilello *et al.*<sup>40</sup> repeated these pharmacodynamics experiments and exposed mixtures of  $10^7$  CEM uninfected cells and  $10^5$  CEM-H9<sub>IIIB</sub>-infected cells (infected-to-uninfected ratio of 1:100) to continuous infusions of 0.5, 1 and 2  $\mu\text{M}$  (representing 4, 8 and 16 times the  $\text{EC}_{50}$ ). Viral infection was assayed in cell-free medium by p24 antigen ELISA while virus spreading was assayed by flow cytometry. Interestingly, the authors also analysed un-integrated HIV-1 DNA by PCR amplification of the DNA in the Hirt-extracted supernatants at 3, 5 and 7 days post infection. These various analyses revealed that HIV-1 replication and spreading is completely inhibited when cells are treated with 0.5  $\mu\text{M}$  A-77003. Although 0.5  $\mu\text{M}$  A-77003 completely inhibited HIV in the hollow fibre, this drug concentration was not clinically effective and could therefore not be used in clinic due to toxicity concerns including phlebitis.<sup>41</sup>

Another protease inhibitor evaluated in the HFIM system against HIV-1 was atazanavir (BMS-232632). In this study by Drusano *et al.*,<sup>42</sup> four hollow-fibre units containing a mixture of HIV-infected (1% of the total cell population) and uninfected cells were infused with atazanavir. In the unit serving as the negative control, only growth medium was circulated. The second unit, serving as the positive control, was continuously infused with  $4\times \text{EC}_{50}$ . In the third unit, atazanavir was circulated with a peak concentration of 56.7 nM at 2 h (with a 5.5 h terminal half-life) producing a 24 h concentration of 3.55 nM and an AUC that was the same as that for the continuous infusion unit. The fourth unit was exposed to atazanavir at a regimen estimated to cause equivalent suppression to the continuous-infusion unit and required a 4-fold higher AUC than that used in the third unit. The intermittent administrations of drug in the third and fourth units were performed daily for the duration of the experiment (9 days of infection). Viral infection was quantified by measuring the amount of p24 antigen released in the supernatants. Although  $4\times \text{EC}_{50}$  administered as a bolus followed by a no-drug washout failed to suppress virus replication past 9 days of infection, virus replication was completely inhibited by continuous infusion at  $4\times \text{EC}_{50}$  and by  $16\times \text{EC}_{50}$  delivered as a bolus followed by a no-drug washout, suggesting that the time above the  $\text{EC}_{50}$  is the linked variable and that  $16\times \text{EC}_{50}$  could completely suppress virus replication if clinically administered on a daily schedule (once-a-day clinical dosing has been confirmed by Sanne *et al.*<sup>43</sup> in a subsequent clinical study).

Similar pharmacodynamic studies have been performed with other HIV-1 inhibitors including: stavudine [2', 3'-didehydro-3'-deoxythymidine (d4T) a nucleoside analogue],<sup>44</sup> abacavir (a nucleoside analogue)<sup>45</sup> and amprenavir in combination with ritonavir (protease

inhibitors),<sup>46</sup> further demonstrating the power of this system as a suitable platform for *in vivo* dose-range and dose-fractionation studies.

### Chikungunya virus (CHIKV)

The lack of antiviral treatment for the mosquito-borne viral disease caused by CHIKV has led Gallegos *et al.*<sup>47</sup> to evaluate the antiviral activities of ribavirin and IFN- $\alpha$  as potential therapeutic options for CHIKV disease treatment. In this study, the authors used the HFIM to experimentally validate the PK/PD model simulations that they performed to predict the anti-CHIKV response associated with ribavirin and IFN- $\alpha$  treatments. Two cellulosic HFBs were inoculated with  $10^8$  Vero cells and 100 pfu of CHIKV. The first cartridge served as a control while the second cartridge received a continuous infusion of a combination of ribavirin and IFN- $\alpha$  at exposures equivalent to 24 h human plasma  $\text{AUC}_{0-24}$ . Supernatants were harvested 24 h after therapy and viral burden was assessed by plaque assay. While this study revealed that the combination of ribavirin and IFN- $\alpha$  at standard clinical regimens can potentially reduce CHIKV levels by 99% 24 h after therapy, it also demonstrated that ribavirin and IFN- $\alpha$  are highly synergistic for the inhibition of CHIKV infection. It equally revealed that the HFIM can be a powerful tool for experimental validation of predicted antiviral activities. Indeed, the PK/PD model simulations used in this study predicted that this antiviral combination would yield a 2.5  $\log_{10}$  reduction in viral burden after 24 h—a prediction that was experimentally validated in the HFIM (a 2.1  $\log_{10}$  reduction in viral burden was observed), highlighting ribavirin/IFN- $\alpha$  combination as a potential therapeutic strategy for the treatment of CHIKV infections. A synergistic interaction between ribavirin and IFN could clinically translate into the use of lower concentrations of each drug in combination for maximal viral inhibition with reduced side effects.

### Dengue virus (DENV) and Zika virus (ZIKV)

Ribavirin and IFN- $\alpha$  drug combination was also assessed by Pires de Mello *et al.*<sup>24</sup> as a potential antiviral therapeutic approach to treat DENV. The authors first determined the  $\text{EC}_{50}$  values of each drug by evaluating their antiviral activity (as single agents or in combination) in confluent monolayers of cells grown in 6-well plates; values were determined over the entire time course of the assay by calculating the AUC for all monotherapy arms. To then examine the effect of the window of treatment initiation on the effectiveness of this drug combination on DENV,  $10^5$  pfu of DENV were mixed with  $10^8$  Huh-7 cells and inoculated into the ECS of a cellulosic HFB. A total of six cartridges were used, with one serving as a no-treatment control. In this experiment, previously known HCV (belonging to the same family as DENV) clinical regimens of IFN- $\alpha$ /ribavirin combination were simulated, and treatment was then initiated at different timepoints post inoculation (0, 2, 6, 12 and 24 h) in the remaining cartridges. Likewise, in another experiment, the authors evaluated the effects of clinical exposures of IFN- $\alpha$ /ribavirin after 24 h post infection. In this case,  $10^8$  Huh-7 cells were mixed with DENV at an moi of 0.001 pfu/cell and inoculated into the ECS of a cellulosic hollow-fibre cartridge. A total of four cartridges were used for this experiment. Twenty-four hours post infection, clinical doses of ribavirin (600 mg twice a day) and IFN (36 million IU twice a day) were administered into the hollow-fibre unit, for 3 days



(either singly or in combination) with one cartridge serving as the no-treatment control. Both experiments were conducted over 3 days, and the ECS of each cartridge was sampled daily and viral burden was quantified by plaque assay on Vero cells.

These experiments revealed that: (i) viral suppression greatly increased with early drug administration; (ii) ribavirin/IFN combination therapy can potentially reduce DENV infection by 99%, even when treatment is administered after 24 h post infection, although ribavirin alone cannot effectively suppress DENV; and (iii) IFN alone inhibited DENV infection to levels similar to the combination regimen, suggesting that the antiviral effects of this combination therapy at inhibiting DENV infection are mostly attributed to IFN alone and the addition of ribavirin could only increase the risk of toxicity. Therefore, IFN as a monotherapy regimen represents a clinically more effective and safer treatment option for DENV infections. It is, however, important to note here that this IFN antiviral activity against DENV was only observed in Huh-7 cells and could not be recapitulated when the experiments were performed on Vero cells. Although Huh-7 cells are of human origin and possess a functional IFN mechanism lacking in Vero cells (IFN-deficient monkey deriving-cells that can respond to exogenous IFN), this specific finding highlights the importance of proper host cell selection when performing preclinical drug evaluations in the HFIM.

Pires de Mello *et al.*<sup>25</sup> equally assessed the broad-spectrum polymerase inhibitor favipiravir in the HFIM for its antiviral properties against ZIKV. The authors began by evaluating the EC<sub>50</sub> concentrations of this compound in a 6-well plate 4 day experiment. Once the EC<sub>50</sub> values were established, drug evaluation was then performed in the HFIM system. Huh-7 cells (10<sup>8</sup>) were mixed with 10<sup>5</sup> pfu of ZIKV (MOI 0.001 pfu/cell) and inoculated into the ECS of a cellulosic hollow-fibre cartridge. A total of six cartridges were used. As one cartridge served as a no-treatment control, favipiravir was administered as a continuous infusion into the remaining five cartridges at concentrations of 0, 31.25, 62.5, 125, 250 and 500 µM for 7 days. In a second experiment, the authors validated their novel deterministic model simulations predicting the viral burden profiles of ZIKV after administration of clinically relevant favipiravir dosage regimens. One cartridge received a 1 h infusion of favipiravir corresponding to a low IAV dose regimen, whereas the second cartridge received a 1 h infusion of favipiravir corresponding to a high Ebola virus dose regimen. The third cartridge received no drug and served as a no-treatment control. All three cartridges were inoculated as previously described. For both types of experiments, viral burden was assessed by plaque assay on Vero cells. To ensure that the desired drug profiles were achieved in the HFIM system, the central reservoir of the HFIM system was sampled daily and drug concentrations were measured by LC-MS/MS.

One technically important remark here is that DMSO, used to solubilize the drug, was maintained in the assay medium at a 1% final concentration (to ensure that favipiravir remained soluble throughout the experiments), and this was also allowed in the no-treatment control. Results of both types of experiments showed that favipiravir can inhibit ZIKV replication in Huh-7 cells in a dose-dependent manner, with 500 µM showing the highest level of inhibition. Both the IAV and the Ebola virus regimens tested in the HFIM were able to reduce ZIKV burden by more than 99% at Day 5 (although the IAV regimen showed a slightly

higher inhibition at Day 7). Additionally, the novel model developed by the authors (MBM model) to predict ZIKV viral burden profiles was consistently validated in the HFIM, again demonstrating its suitability as an alternative 'in vivo-like' system for drug evaluations. Although the Ebola regimen simulated in this study represents a more effective therapeutic approach that could be clinically used for the treatment of ZIKV-infected patients, the issues related to drug toxicity of such high drug exposures need to be fully investigated for this regimen to be implemented in clinics. Nevertheless, the low-dose influenza regimen, which is nearly half the exposure of the Ebola regimen, offers a safer and still effective therapeutic option presenting less drug-related toxicity, if the treatment is initiated at early stages of infection.

### **Vaccinia virus (VV)**

A pharmacodynamic study on cidofovir (a phosphonate nucleotide drug) in the HFIM system has also been conducted by McSharry *et al.*<sup>26</sup> Cidofovir is a viral DNA polymerase inhibitor currently approved for use against cytomegalovirus retinitis and for the emergency treatment of smallpox or complications following vaccination. In this study by McSharry *et al.*,<sup>26</sup> four viral strains of VV were tested. The EC<sub>50</sub> for cidofovir for each viral strain was first determined on HeLa-S3 cell monolayers, grown in 25 cm<sup>2</sup> tissue culture plasticware, and infected at an MOI of 0.01 pfu/cell and treated with various concentrations of cidofovir 3 to 5 days post infection (depending on the viral strain being tested), viral burden was estimated by plaque assay as previously described by Earl *et al.*<sup>48</sup> To demonstrate viral growth in the hollow fibre, a 25 mL mixture of 10<sup>8</sup> uninfected HeLa-S3 cells and 10<sup>6</sup> VV-infected HeLa-S3 cells was injected into the ECS of each of the three different polysulfone hollow-fibre cartridge (20 kDa MWCO) units used for this purpose (each unit corresponding to each VV strain). Viral growth was then measured by plaque assay on the cell-free supernatant sampled from the ECS over 4 days of infection. Given that the VV-WR strain expressed the HIV p24 antigen following infection, p24 ELISA was also performed to quantify viral release with this specific strain. A similar procedure was used for dose-range studies, in which media containing various concentrations of cidofovir (0, 12.5, 25, 50, 100 and 200 µM) were pumped as continuous infusions in six different hollow-fibre units over 3 days. For dose-fractionation studies, cidofovir was infused into the central reservoir either as a bolus or as a continuous infusion. Boluses (or intermittent exposures) were administered over a 1 h period followed by a no-drug washout (to simulate normal human half-life). A total of two dose-fractionation studies were performed and actual cidofovir concentrations in each HFIM system at each timepoint were determined and monitored by LC-MS.

All three VV strains used in this study grew well in the HFIM system, with the IHD-J strain yielding the highest virus titre at the end of the experiment (4 days post infection.). When administered as a continuous infusion, cidofovir was only able to completely suppress VV replication at 200 µM (with 50% inhibition caused by approximately 38 µM), suggesting that larger exposures (AUC) of this drug are required to substantially reduce viral titres, which therefore raises important clinical questions related to its toxicological safety profile. It is important to note here that

the licensed dose of cidofovir is 5 mg/kg. It is thus interesting to see that 3  $\mu\text{M}$  continuous infusion of cidofovir (corresponding to a 10 mg/kg dose of cidofovir with an  $\text{AUC}_{0-24}$  of 72  $\mu\text{M}\cdot\text{h}$ ) failed to significantly inhibit viral replication in this HFIM system, suggesting that the licensed 5 mg/kg dose might also not have any significant antiviral effect against this virus (suggesting that further *in vivo* studies in animal models need to be performed).

Although the authors only reported the results of the first dose-fractionation study for the VV-WR strain, it would have been interesting to see if these findings also held for the two other VV strains mentioned in the study. The fact that the authors found no substantial difference in antiviral effect between both drug administration profiles (boluses and continuous infusions) led them to conclude that the pharmacodynamically linked variable for cidofovir for VV is the  $\text{AUC}/\text{EC}_{50}$ , meaning that the antiviral effect observed at higher doses could also be independent of the route of administration of the drug.

With the HFIM, it is therefore possible to determine the dosage and the spacing regimen allowing maximal viral suppression during infection. The effects of interindividual variability on the pharmacokinetics of some antiviral compounds can also be simulated using this system. This alternative '*in vivo*-like' system for drug evaluations therefore stands as a powerful tool for experimental validation of predicted antiviral activities, although for some antiviral compounds presenting high pharmacokinetic variability such as raltegravir, further clinical studies might still be required to confirm the evaluated drug dosing and treatment regimens.

## Discussion

Given the scarcity of the literature describing the applications of the HFIM system for viral infection studies, we undertook this work to provide researchers in this field with some of the necessary technical knowledge surrounding the use of the HFIM system for studies involving eukaryotic viruses, of mostly human importance. As pointed out by Sadouki *et al.*,<sup>2</sup> there is wide variability in the reporting of most HFIM system studies, which we also noticed when editing the current research work. Our work therefore also aimed at summarizing the different infection approaches as well as readouts described in the available literature for the use of this system in eukaryotic viral infection studies.

As the HFIM system can be used in specific types of infection studies, a few recommendations can be considered when employing this system. As best practice before performing any infections in the HFIM system, it is recommended to initially perfuse the system and the cartridges with PBS for at least 2 days, followed by an additional 24 h treatment with cell growth medium, as reported by McSharry *et al.*<sup>38</sup> and Pihl *et al.*<sup>30</sup> This procedure will allow for the removal of any residues (probably resulting from the hydrophobic coating of the fibres and the manufacturing process of the cartridges) that could be toxic to the cells seeded in the cartridges. Additionally, since it is important to attempt to mimic a host natural *in vivo* infection, we also recommend initiating viral infections in the HFIM system by mixing virus-infected and non-infected cells before inoculation into the hollow-fibre cartridge. This procedure has been documented in most of the studies reported in this review. As the MOI used for the infection in this system seems to greatly depend on the type of study to be carried out, it is therefore logical

to use high MOI (for instance 5–10) for viral expansion studies and low MOI (for instance 0.001) for drug resistance and PK/PD studies.

High MOI infections often provide viruses with increased genetic diversity, which in turn increases the chances of drug escape mutants. Moreover, drug resistance (or at least reduced drug susceptibility) resulting from high MOI infection (for both cell-to-cell infection and cell-free virus infection) has been reported during HIV-1 treatment with the NRTI tenofovir,<sup>49</sup> possibly explaining why low MOI would be adequate when conducting drug resistance and PK/PD studies.

During viral expansion studies, it is possible that the amount of serum contained in the media might affect the amount of virus recovered at the end of the study, as observed by Leong *et al.*<sup>21</sup> and Pihl *et al.*<sup>30</sup> Although in the Pihl *et al.*<sup>30</sup> study serum-free media (AEM) yielded the highest virus titres ( $2.4 \times 10^9$  ffu), 15% FCS-containing medium has equally been demonstrated to yield high titres of HIV p24 antigen by Leong *et al.*,<sup>21</sup> despite the fact that other parameters such as IL-2 concentrations and glucose content also accounted for this high yield in this later study. Therefore, the choice of medium composition should be guided by the growth requirements of the cell type used for the study.

Leong *et al.*<sup>21</sup> also found that 5 kDa MWCO bioreactor cartridges generated lower p24 yields than 20 kDa MWCO cartridges, a finding which suggests that the choice of the MWCO of the cartridge might have an impact on the viral yield. We have nevertheless noticed that most studies reviewed in this work reported using 20 kDa MWCO cartridges. Most studies reported using polysulfone cartridges, which appear to be specifically good for cell culture as they allow better cell growth and high cell densities of both adherent and suspension cells.<sup>5,50</sup> Nonetheless, few studies have also reported a successful use of cellulose cartridges.<sup>24,25,47</sup> Even though this type of cartridge is not recommended for mammalian cell culture,<sup>5,50</sup> they are, however, suitable for use in antibiotic PK/PD applications as well as *in vitro* toxicology studies, especially if the compound under study has a greater binding affinity for polysulfone hollow-fibre membranes than cellulosic hollow-fibre membranes, therefore reducing its distribution and availability throughout the entire HFIM system. We have summarized in Table 1 the different aspects surrounding the use of the HFIM system for eukaryotic viral studies.

As nutrients are continuously pumped through the system to support cell growth, antiviral agents can be added and removed at a rate that simulates human pharmacokinetic patterns for the antiviral agent. With this system, it is therefore possible to simulate interpatient pharmacokinetic variability by altering the clearance<sup>39</sup> and the half-life of the drug under study. While dosing is commonly achieved with automated or manual syringe drivers, simulations of IV boluses or continuous infusions can be done by adding the drugs to either the diluent reservoir (continuous infusion) or the central reservoir (IV bolus).

Pihl *et al.*<sup>30</sup> addressed a few important features related to the biology of viruses grown in the HFIM system. Long-term culture and passaging of some viruses in tissue culture plates have sometimes led to their adaptation and attenuation (also characterized by a loss of pathogenicity). By sequencing the entire coding sequence of HCV, Pihl *et al.*<sup>30</sup> demonstrated that HCV grown in HFBs presented a very high genetic stability as well as a very low

**Table 2.** Hollow-fibre advantages and disadvantages with eukaryotic virus cultures

Advantages	Disadvantages
<ul style="list-style-type: none"> <li>• Allows higher density cell cultures (up to <math>10^9</math> cells)</li> <li>• Extended duration experiments possible (up to 2 months) without the need to divide the cells</li> <li>• Closed sterile system</li> <li>• Allows controlled drug concentrations to be monitored</li> <li>• Can accurately mimic PK/PD of target drug compounds</li> <li>• No immune system—could replace immunocompromised animal models</li> <li>• Continuous sampling of cultures over time (as well as multiple harvest of the virus)</li> <li>• Can be used to express and purify proteins</li> <li>• Controllable protein size exclusion</li> <li>• Relatively inexpensive compared with clinical studies</li> <li>• Can be used to monitor the emergence of drug-resistant viruses, as well as drug concentrations, allowing the emergence of these drug-resistant viruses</li> <li>• Could be used to replace humans (or <i>in vivo</i> animal models) in trials for antiviral compounds showing efficacy against viruses usually associated with high mortality and morbidity</li> <li>• Can successfully predict the exposure response and schedule response identical to those reported in clinical trials</li> </ul>	<ul style="list-style-type: none"> <li>• Hard to maintain sterility</li> <li>• Maintenance of liquid-tight integrity can be difficult</li> <li>• Assembly is challenging</li> <li>• Technically complex system with lots of pumps and tubing, not so user friendly unless training is provided</li> <li>• Requires large amount of medium and reagents</li> <li>• Most intracellular processes cannot be visualized</li> <li>• System restricted to specific types of studies</li> <li>• Does not account for immune system response</li> <li>• Adherence of cells to fibres/filter module could make quantification difficult</li> <li>• Some drugs adhere to polycarbonate module shell—pharmacokinetics testing required for each drug to ensure correct <math>C_{max}</math> is achieved</li> <li>• Dosage regimens estimated in this system may still require further <i>in vivo</i> validations for certain compounds</li> </ul>

level of heterogeneity (of the viral population) from the early to the late harvests (with only a slight increase in heterogeneity over time). Moreover, HCV grown in HFBS exhibited similar characteristics as the ones grown in cell cultures (similar density, spreading kinetics, infectivity titres, and sensitivity to neutralization with human monoclonal IgG). Although their study was limited to HCV, it is also possible that these findings apply to other viruses, especially when considering that the HFIM system allows the cells to be cultured at densities close to *in vivo*-like conditions, without the need for cell division, which is one of the many advantages of this system that we have summarized in Table 2, together with its disadvantages. Additionally, the system allows serial evaluation of drug exposure profiles, as well as drug efficacy (as previously mentioned), of antiviral compounds at concentration–time profiles identical to that achievable in humans.

The HFIM system is a closed system, meaning that most intracellular processes cannot be visualized. This limitation greatly restricts its applications to only specific types of studies where only the cellular products released in the ECS can be assessed and monitored. Similarly, the biology of some cell lines or viruses (especially those not chronically infecting cells), might favour more a cell-to-cell spreading mechanism, rendering this system not suitable for use for all types of viruses or cells, since the virus (or the cellular product to be assessed) must be released in the ECS for viral quantification to be performed. Furthermore, unlike in a natural host infection scenario, this *in vitro* system is devoid of most immune components often found in natural hosts (except for innate immune mechanisms deployed by cells capable of mounting an interferon antiviral response, with the exception of Vero cells, which lack interferon response). Therefore, viral infection kinetics in this system are certainly different than those occurring in human clinical studies. Nevertheless, the

model more closely represents infections in immunocompromised individuals, presenting an impaired immune system devoid of immune cells and where resistant infections are often more prevalent.

Despite the robustness of this system at accurately simulating clinically achievable concentrations of antivirals, some dosage and drug regimens evaluated in this system failed to be clinically achievable, as previously seen for the oseltamivir/zanamivir combination,<sup>34</sup> raltegravir<sup>39</sup> and the protease inhibitor A-77003.<sup>40</sup> The mechanism of action of the antiviral compound (strong or weak binding to the active site, conformational change of the compound prior to binding), its mode of administration, its rate of adsorption, its bioavailability and distribution, its natural tissue target, its half-life, as well as interindividual variability of the pharmacokinetics of some antiviral compounds, are all possible factors capable of influencing the clinical validation of some of the antiviral activities of some compounds predicted in the HFIM system, which therefore hinder the translation of the predicted dose regimens into clinical practice. This means that human clinical studies might still be needed to validate and confirm the antiviral concentrations predicted in this system. Moreover, the experiments performed in the HFIM system might even also need to be repeated in more than one cell line. Indeed, as observed by Pires de Mello *et al.*,<sup>25</sup> IFN antiviral activity against DENV in this system for instance, could only be observed with Huh-7 cells and could not be recapitulated with Vero cells. Although differences in the biology of these two cell lines, as mentioned above, is a possible explanation for this inconsistency, the fact that this system may not be suitable for all eukaryotic cell types can also not be completely ruled out. Nonetheless, this system represents a great tool to evaluate the efficacy of antiviral compounds targeting

viruses associated with high morbidity and mortality and for which humans (or animal models) cannot be used in clinical studies.

## Acknowledgements

We are indebted to Zahra Sadouki (University College London—Institute for Global Health and Centre of Clinical Microbiology) for her help with gathering the literature and for her advice during manuscript preparation. J.E.K.R.'s research work on hollow fibres at University College London—Institute for Child Health, was partly supported by the National Institute of Health Research (NIHR)—Great Ormond Street Hospital Biomedical Research Centre (GOSH-BRC) (NIHR—GOSH-BRC) (award #20IA27). J.F.S. received funding from the UK Medical Research Council (MR/X0047224/1)

## Transparency declarations

The authors declare no competing interests.

## References

- Knazek RA, Gullino PM, Kohler PO *et al.* Cell culture on artificial capillaries: an approach to tissue growth *in vitro*. *Science* 1972; **178**: 65–7. <https://doi.org/10.1126/science.178.4056.65>
- Sadouki Z, McHugh TD, Aarnoutse R *et al.* Application of the hollow fibre infection model (HFIM) in antimicrobial development: a systematic review and recommendations of reporting. *J Antimicrob Chemother* 2021; **76**: 2252–9. <https://doi.org/10.1093/jac/dkab160>
- Cadwell J. The hollow fibre infection model: principles and practice. *Adv Antibiotics Antibodies* 2015; **1**: 101.
- Bulitta JB, Hope WW, Eakin AE *et al.* Generating robust and informative nonclinical *in vitro* and *in vivo* bacterial infection model efficacy data to support translation to humans. *Antimicrob Agents Chemother* 2019; **63**: e02307–18. <https://doi.org/10.1128/AAC.02307-18>
- KD BIO. FiberCell Hollow Fibre cartridges. <https://www.kdbio.com/products/hollow-fiber-cartridges/>.
- Handa-Corrigan A, Nikolay S, Fletcher D *et al.* Monoclonal antibody production in hollow-fiber bioreactors: process control and validation strategies for manufacturing industry. *Enzyme Microb Technol* 1995; **17**: 225–30. [https://doi.org/10.1016/0141-0229\(94\)00012-G](https://doi.org/10.1016/0141-0229(94)00012-G)
- Gorter A, van de Griend RJ, van Eendenburg JDH *et al.* Production of bi-specific monoclonal antibodies in a hollow-fibre bioreactor. *J Immunol Methods* 1993; **161**: 145–50. [https://doi.org/10.1016/0022-1759\(93\)90289-J](https://doi.org/10.1016/0022-1759(93)90289-J)
- Chu L, Robinson DK. Industrial choices for protein production by large-scale cell culture. *Curr Opin Biotechnol* 2001; **12**: 180–7. [https://doi.org/10.1016/S0958-1669\(00\)00197-X](https://doi.org/10.1016/S0958-1669(00)00197-X)
- Ryll T, Lucki-Lange M, Jäger V *et al.* Production of recombinant human interleukin-2 with BHK cells in a hollow fibre and a stirred tank reactor with protein-free medium. *J Biotechnol* 1990; **14**: 377–92. [https://doi.org/10.1016/0168-1656\(90\)90120-Z](https://doi.org/10.1016/0168-1656(90)90120-Z)
- Singh R, Almutairi M, Alm RA *et al.* Ceftriaxone efficacy against high-MIC clinical *Staphylococcus aureus* isolates in an *in vitro* hollow-fibre infection model. *J Antimicrob Chemother* 2017; **72**: 2796–803. <https://doi.org/10.1093/jac/dkx214>
- VanScoy BD, Trang M, McCauley J *et al.* Pharmacokinetics-pharmacodynamics of a novel  $\beta$ -lactamase inhibitor, CB-618, in combination with meropenem in an *in vitro* infection model. *Antimicrob Agents Chemother* 2016; **60**: 3891–6. <https://doi.org/10.1128/AAC.02943-15>
- Grasso S, Meinardi G, De Carneri I *et al.* New *in vitro* model to study the effect of antibiotic concentration and rate of elimination on antibacterial activity. *Antimicrob Agents Chemother* 1978; **13**: 570–6. <https://doi.org/10.1128/AAC.13.4.570>
- Drusano GL, Sgambati N, Eichas A *et al.* Effect of administration of moxifloxacin plus rifampin against *Mycobacterium tuberculosis* for 7 of 7 days versus 5 of 7 days in an *in vitro* pharmacodynamic system. *mBio* 2011; **2**: e00108–11. <https://doi.org/10.1128/mBio.00108-11>
- Garimella N, Zere T, Hartman N *et al.* Effect of drug combinations on the kinetics of antibiotic resistance emergence in *Escherichia coli* CFT073 using an *in vitro* hollow-fibre infection model. *Int J Antimicrob Agents* 2020; **55**: 105861. <https://doi.org/10.1016/j.ijantimicag.2019.105861>
- Heffernan AJ, Sime FB, Naicker S *et al.* Pharmacodynamics of once-versus twice-daily dosing of nebulized amikacin in an *in vitro* hollow-fiber infection model against 3 clinical isolates of *Pseudomonas aeruginosa*. *Diagn Microbiol Infect Dis* 2021; **100**: 115329. <https://doi.org/10.1016/j.diagmicrobio.2021.115329>
- Carr D, Zhang Z, Si Q *et al.* *In vitro* hollow-fiber studies assessing antibacterial activity of ceftolozane/tazobactam against multidrug-resistant *Pseudomonas aeruginosa*. *Open Forum Infect Dis* 2020; **7**: ofaa469. <https://doi.org/10.1093/ofid/ofaa469>
- Portillo-Calderón I, Ortiz-Padilla M, de Gregorio-Iaria B *et al.* Activity of fosfomycin and amikacin against fosfomycin-heteroresistant *Escherichia coli* strains in a hollow-fiber infection model. *Antimicrob Agents Chemother* 2021; **65**: e02213–20. <https://doi.org/10.1128/AAC.02213-20>
- Garcia E, Diep JK, Sharma R *et al.* Evaluation strategies for triple-drug combinations against carbapenemase-producing *Klebsiella pneumoniae* in an *in vitro* hollow-fiber infection model. *Clin Pharmacol Ther* 2021; **109**: 1074–80. <https://doi.org/10.1002/cpt.2197>
- Montero M, VanScoy BD, López-Causapé C *et al.* Evaluation of ceftolozane-tazobactam in combination with meropenem against *Pseudomonas aeruginosa* sequence type 175 in a hollow-fiber infection model. *Antimicrob Agents Chemother* 2018; **62**: e00026–18. <https://doi.org/10.1128/AAC.00026-18>
- VanScoy BD, Scangarella-Oman NE, Fikes S *et al.* Relationship between gepotidacin exposure and prevention of on-therapy resistance amplification in a *Neisseria gonorrhoeae* hollow fiber *in vitro* infection model. *Antimicrob Agents Chemother* 2020; **64**: e00521–20. <https://doi.org/10.1128/AAC.00521-20>
- Leong M, Babbitt W, Vyas G. A hollow-fiber bioreactor for expanding HIV-1 in human lymphocytes used in preparing an inactivated vaccine candidate. *Biologicals* 2007; **35**: 227–33. <https://doi.org/10.1016/j.biologicals.2007.04.002>
- Hirschel M, Gangemi JD, McSharry J *et al.* Novel uses for hollow fiber bioreactors. *Genet Eng Biotechnol News* 2011; **31**: 42–4. <https://doi.org/10.1089/gen.31.12.16>
- Piret J, Cooney C. Immobilized mammalian cell cultivation in hollow fiber bioreactors. *Biotechnol Adv* 1990; **8**: 763–83. [https://doi.org/10.1016/0734-9750\(90\)91996-T](https://doi.org/10.1016/0734-9750(90)91996-T)
- Pires de Mello CP, Drusano GL, Rodriguez JL *et al.* Antiviral effects of clinically-relevant interferon- $\alpha$  and ribavirin regimens against dengue virus in the hollow fiber infection model (HFIM). *Viruses* 2018; **10**: 317. <https://doi.org/10.3390/v10060317>
- Pires de Mello CP, Tao X, Kim TH *et al.* Clinical regimens of favipiravir inhibit Zika virus replication in the hollow-fiber infection model. *Antimicrob Agents Chemother* 2018; **62**: e00967–18. <https://doi.org/10.1128/AAC.00967-18>
- McSharry JJ, Deziel MR, Zager K *et al.* Pharmacodynamics of cidofovir for vaccinia virus infection in an *in vitro* hollow-fiber infection model system. *Antimicrob Agents Chemother* 2009; **53**: 129–35. <https://doi.org/10.1128/AAC.00708-08>

- 27** Gardner TA, Ko SC, Yang L *et al.* Serum-free recombinant production of adenovirus using a hollow fiber capillary system. *Biotechniques* 2001; **30**: 422–8. <https://doi.org/10.2144/01302pf01>
- 28** Graham FL, Prevec L. Methods for construction of Adenovirus vector. *Mol Biotechnol* 1995; **3**: 207–20. <https://doi.org/10.1007/BF02789331>
- 29** Tapia F, Vogel T, Genzel Y *et al.* Production of high-titer human influenza A virus with adherent and suspension MDCK cells cultured in a single-use hollow fiber bioreactor. *Vaccine* 2014; **32**: 1003–11. <https://doi.org/10.1016/j.vaccine.2013.11.044>
- 30** Pihl AF, Offersgaard AF, Mathiesen CK *et al.* High density Huh7.5 cell hollow fiber bioreactor culture for high-yield production of hepatitis C virus and studies of antivirals. *Sci Rep* 2018; **8**: 17505. <https://doi.org/10.1038/s41598-018-35010-5>
- 31** Strasfeld L, Chou S. Antiviral drug resistance: mechanisms and clinical implications. *Infect Dis Clin North Am* 2010; **24**: 413–37. <https://doi.org/10.1016/j.idc.2010.01.001>
- 32** Brown AN, McSharry JJ, Weng Q *et al.* *In vitro* system for modelling influenza A virus resistance under drug pressure. *Antimicrob Agents Chemother* 2010; **54**: 3442–50. <https://doi.org/10.1128/AAC.01385-09>
- 33** Vere Hodge A, Field HJ. Chapter 13 - General mechanisms of antiviral resistance. In: Tibayrenc M, ed. *Genetics and Evolution of Infectious Disease*. Elsevier, 2011; 339–62. <https://doi.org/10.1016/B978-0-12-384890-1.00013-3>
- 34** Pires de Mello CP, Drusano GL, Adams JR *et al.* Oseltamivir-zanamivir combination therapy suppresses drug-resistant H1N1 influenza A viruses in the hollow fiber infection model (HFIM) system. *Eur J Pharm Sci* 2018; **111**: 443–9. <https://doi.org/10.1016/j.ejps.2017.10.027>
- 35** Brown AN, McSharry JJ, Weng Q *et al.* Zanamivir at 600 milligrams twice daily, inhibits oseltamivir-resistant 2009 pandemic H1N1 influenza virus in an *in vitro* hollow-fiber infection model system. *Antimicrob Agents Chemother* 2011; **55**: 1740–6. <https://doi.org/10.1128/AAC.01628-10>
- 36** Mehrotra N, Gupta M, Kovar A *et al.* The role of pharmacokinetics and pharmacodynamics in phosphodiesterase-5 inhibitor therapy. *Int J Impot Res* 2007; **19**: 253–64. <https://doi.org/10.1038/sj.ijir.3901522>
- 37** McSharry JJ, Drusano GL. Antiviral pharmacodynamics in the hollow fibre bioreactors. *Antivir Chem Chemother* 2011; **21**: 183–92. <https://doi.org/10.3851/IMP1770>
- 38** McSharry JJ, Weng Q, Brown A *et al.* Prediction of the pharmacodynamically linked variable of oseltamivir carboxylate for influenza A virus using an *in vitro* hollow-fiber infection model system. *Antimicrob Agents Chemother* 2009; **53**: 2375–81. <https://doi.org/10.1128/AAC.00167-09>
- 39** Brown AN, Adams JR, Baluya DL *et al.* Pharmacokinetic determinants of virological response to raltegravir in the *in vitro* pharmacodynamic hollow-fiber infection model system. *Antimicrob Agents Chemother* 2015; **59**: 3771–7. <https://doi.org/10.1128/AAC.00469-15>
- 40** Bilello JA, Bilello PA, Kort JJ *et al.* Efficacy of constant infusion of A-77003, an inhibitor of the human immunodeficiency virus type 1 (HIV-1) protease, in limiting acute HIV-1 infection *in vitro*. *Antimicrob Agents Chemother* 1995; **39**: 2523–7. <https://doi.org/10.1128/AAC.39.11.2523>
- 41** Reedijk M, Boucher CAB, van Bommel T *et al.* Safety, pharmacokinetics, and antiviral activity of A77003, a C2 symmetry-based human immunodeficiency virus protease inhibitor. *Antimicrob Agents Chemother* 1995; **39**: 1559–64. <https://doi.org/10.1128/AAC.39.7.1559>
- 42** Drusano GL, Bilello AJ, Preston LS *et al.* Hollow-fiber unit evaluation of a new human immunodeficiency virus type 1 protease inhibitor, BMS-232632, for determination of the linked pharmacodynamic variable. *J Infect Dis* 2001; **183**: 1126–9. <https://doi.org/10.1086/319281>
- 43** Sanne I, Piliero P, Squires K *et al.* Results of a phase 2 clinical trial at 48 weeks (AI424-007): a dose ranging, safety, and efficacy comparative trial of atazanavir at three doses in combination with didanosine and stavudine in antiretroviral-naïve subjects. *J Acquir Immune Defic Syndr* 2003; **32**: 18–29. <https://doi.org/10.1097/00126334-200301010-00004>
- 44** Bilello JA, Bauer G, Dudley MN *et al.* Effect of 2',3'-didehydro-3'-deoxythymidine in an *in vitro* hollow-fiber pharmacodynamic model system correlates with results of dose-ranging clinical studies. *Antimicrob Agents Chemother* 1994; **38**: 1386–91. <https://doi.org/10.1128/AAC.38.6.1386>
- 45** Drusano GL, Bilello PA, Symonds WT *et al.* Pharmacodynamics of abacavir in an *in vitro* hollow fiber model system. *Antimicrob Agents Chemother* 2002; **46**: 464–70. <https://doi.org/10.1128/AAC.46.2.464-470.2002>
- 46** Preston SL, Piliero PJ, Bilello JA *et al.* *In vitro-in vivo* model for evaluating the antiviral activity of amprenavir in combination with ritonavir administered at 600 and 100 milligrams, respectively every 12 hours. *Antimicrob Agents Chemother* 2003; **47**: 3393–9. <https://doi.org/10.1128/AAC.47.11.3393-3399.2003>
- 47** Gallegos KM, Drusano GL, D'Argenio DZ *et al.* Chikungunya virus: *in vitro* response to combination therapy with ribavirin and interferon alfa 2a. *J Infect Dis* 2016; **214**: 1192–7. <https://doi.org/10.1093/infdis/jiw358>
- 48** Earl PL, Cooper N, Wyatt LS *et al.* Preparation of cell cultures and vaccinia virus stocks. *Curr Protoc Mol Biol* 2001; Chapter 16: Unit 16.16. <https://doi.org/10.1002/0471142727.mb1616s43>
- 49** Law KM, Satija N, Esposito AM *et al.* Cell-to-cell spread of HIV and viral pathogenesis. *Adv Virus Res* 2016; **95**: 43–85. <https://doi.org/10.1016/bs.aivir.2016.03.001>
- 50** FiberCell Systems. Cartridges. <https://www.fibercellsystems.com/products/cartridges/>.